FIRST-PRINCIPLES CALCULATIONS OF YTTRIUM TANTALATE AND NIOBATE CRYSTALS

M. Nazarov[1], L. Th. Leng[2], Y. T. Leong[3], L. L. Chen[2], and I. D. Arellano[4]

[1] Institute of Applied Physics, Academy Sciences of Moldova, Republic of Moldova
[2] Faculty of Engineering and Technology, Multimedia University, Jalan Ayer Keroh Lama, 75450 Melaka, Malaysia
[3] School of Physics, University Sains Malaysia, 11800 USM, Penang, Malaysia
[4] Department of Physics, Technological University of Pereira, Vereda La Julita, Pereira, Colombia.
E-mail address: mvnazarov@mail.ru (Mihail Nazarov)

(Received March 10, 2014)

Abstract

The structural and electronic properties of yttrium tantalate ($YTaO_4$) and yttrium niobate ($YNbO_4$) crystals are studied using experimental and first-principles GGA+*U* total energy calculations. The band gap of the host lattice from absorption and luminescence experiment is measured to be 5.1 eV for $YTaO_4$ and 4.1eV for $YNbO_4$. This is close to 5.14 eV and 4.28 eV, respectively, reproduced by means of GGA+*U* approach. In our calculation, we tune both Hubbard energy *U* and exchange parameter *J* to reproduce the energy gap measured experimentally. It is found that Hubbard energy *U* plays a major role in reproducing the experimentally measured energy gap, but exchange parameter *J* does not. We also calculate the density of states (DOS) using the optimized *U* to interpret the experimentally measured luminescence spectra. Both the experimental and DOS calculations show that the valence band of tantalate (Ta) and niobate (Nb) systems is mainly composed of oxygen (O) 2p states. The lower conduction band is mainly composed of Ta 5d states or Nb 4d states, respectively, while the upper conduction band involves the contribution mainly from yttrium (Y) 4d states, with the middle conduction band mainly a mixture of Ta or Nb and Y states. The calculated partial DOS of each atom in the tantalate and niobate system is then compared with the UV and VUV spectra from photoluminescence excitation (PLE) experiment to explain the nature of the bands observed.

1. Introduction

Undoped $YTaO_4$ and $YNbO_4$ are well known as self-activated phosphors for more than four decades. Even though these materials are well-known self-activated phosphors, their electronic structure, optical absorption mechanism, and optical transitions have not been clearly understood.

Historically, Ferguson [1] in 1957 was the first to describe both natural fergusonite (a yttrium niobium-tantalate) as well as synthetic $YTaO_4$ correctly, where they crystallized in monoclinic symmetry with the space group 15 ($I\,2/a$). $YTaO_4$ exhibits three crystal structures. At high temperature the tetragonal form (T, space group 88) with scheelite structure distorts via a second-order phase transition to monoclinic (M, space group 15) structure having the fergusonite structure. Another monoclinic structure, called M′ (space group 13), can be synthesized directly

at lower temperatures (below 1400°C). M′ transforms to T at approximately 1450°C and then to M upon cooling. $YNbO_4$ has a polymorphism and exhibits two polymorphs: the high temperature T-scheelite and the low temperature M-fergusonite [2-5]. At high-temperature tetragonal form (T) of $YNbO_4$ with scheelite structure distorts via a second-order phase transition to a monoclinic (M) structure having the fergusonite structure. The monoclinic phase transforms into tetragonal phase at 900°C.

$YNbO_4$, together with $YTaO_4$, are commercially valuable and used extensively in X-ray intensifying screens. As we all know, performances of phosphors and luminescence properties strongly depend on their crystal and electronic structures which can be understood via quantum mechanical calculations. Some fundamental questions concerning host lattice emission and charge transfer transitions in $YTaO_4$ and $YNbO_4$ remain to be answered. To better understand the luminescence mechanism, crystallographic structure, and absorption mechanism of these phosphors, first-principles calculations have been carried out.

This paper is dedicated to investigate the electronic properties of yttrium tantalate and niobate systems through the study of its density of states (DOS) and band structure using experimental and first-principles calculations. To the best of our knowledge, there is no offer of any explanation in the literature to the apparent discrepancy between the experimental spectra and calculated DOS [6–9]. The experimental spectra for $YTaO_4$ recorded a 5.1-eV band gap between conduction band and valence band, while the gaps from first-principles calculations are 4.2 eV (without scissor operator) and 4.8 eV (with scissor operator) [6, 10]. Thus, there is a discrepancy of 0.9 eV (without scissor operator) between experiment measurement and first-principles calculation. A scissor operator is applied to include the effects of self-energy and excitonic shift only. Therefore, the band gap issue cannot be resolved even with a scissor operator. Similarly, for $YNbO_4$, from our experimental spectra, we have the band gap between conduction and valence band of 4.1 eV, while the DOS from calculations in [6, 10] infers a band gap of 3.8 eV (value calculated without using the scissor treatment).

Density functional theory (DFT) is a widely used method to calculate the ground state energy of a system by mapping a multiple-electron system into a single electron problem. By incorporating an exchange-correlation, such as a local (spin) density approximation (L(S)DA) and generalized gradient approximations (GGA), DFT has attained much success in deriving the ground state electronic structure properties. However, when it comes to systems with highly correlated electrons, such as that possessing d- or f-electrons, computations with L(S)DA or GGA reveal their disadvantages. They fail to describe magnetic insulators, such as 3d-transition-metal oxides or Mott insulator. Despite being able to reproduce the ground state structures for the magnetic NiO and MnO series, the theory wrongly predicted Mott insulators as metal. In addition, the gaps in NiO and MnO are predicted to be too small in magnitude compared to photoemission experiments [11]. Many attempts have been made to improve the L(S)DA and GGA calculations on systems with d- or f-electrons. One of the most successful improvements is the '+*U*' approach (i.e., L(S)DA+*U* and GGA+*U*). As pointed out by Anisimov et al. [12, 13], the L(S)DA behaves like a weak-coupling mean-field theory. Anisimov et al. generalized the L(S)DA method by proposing the L(S)DA+*U* approach to strongly correlated systems. In this approach, effective on-site interactions are introduced to the existing Hamiltonian to better account for the orbital dependence of the Coulomb and exchange interactions of the strongly correlated (i.e., d- and f-) electrons. The basic idea of L(S)DA+*U* (which also applies to GGA+*U*) calculation is described as follows [12–14]. For delocalized s- and p-electrons in the atom, only L(S)DA calculations are involved. For localized d- or f-electrons, a on-site d-d column

interaction or a Hubbard-like term is used instead of the averaged coulomb energy. The d- or f-electron interactions can be quite accurately calculated via this '+U' approach. Many DFT packages, such as WIEN2k [15], provide computational functionality to conveniently calculate the '+U' effect.

The discrepancy between the published experimental results on the energy band gap of $YTaO_4$ and $YNbO_4$ from luminescence excitation spectra or absorbance data and that calculated from DFT is significant. One of the main goals of this work is to address this issue by reproducing the experimentally measured energy band gap through GGA+U calculations using the DFT package WIEN2k [15]. DOS obtained from the GGA+U calculation is then used to provide insight into the origin of the features measured in the excitation spectra.

2. Experimental and theoretical methods

2.1. Sample preparation

A few sets of yttrium tantalate and niobate phosphors were prepared by solid state reaction method from a homogeneous mixture consisting of Y_2O_3 (99.9%) and Ta_2O_5 or Nb_2O_5 (Optipur). Different inorganic salts, such as Li_2SO_4, LiCl, and Na_2SO_4, were used as a flux. The mixtures were homogenized with a ball mill, in acetone medium, and dried at 70°C. The phosphor samples were baked at 1200°C for 4 h and slowly cooled to room temperature. Finally, the samples were water washed, dried, and then sieved.

2.2. Characterization techniques

The samples were investigated using X-ray diffraction, UV and VUV excitation luminescence, and first-principles quantum-mechanical calculations in order to study their structural and luminescent properties.

UV measurements were monitored using a Perkin-Elmer LS50B spectrometer with a xenon flash lamp. VUV excitation spectra of samples were measured using a VUV spectrophotometer equipped with a VUV monochromator (ARC, VM 502) and a light source of a 30-W deuterium lamp (ARC, DS775-100).

In XRD measurements, a Cu-Kα radiation (λ = 1.54 Å) source generated from a Rigaku rotating anode generator was used operating at 40 kV and 40 mA. Basically, we measured the powder diffraction profiles (Θ–2Θ scan) in a range of 10° to 80°.

2.3. Ab initio method

Calculations were conducted using the all-electron full potential linearized augmented plane-wave method (FP-LAPW) [16–18] as implemented in WIEN2k [15]. In the FP-LAPW method, the unit cell is divided into non-overlapping atomic spheres, or Muffin-tin spheres that centered at the atomic sites and the interstitial region. In the interstitial region, a plane wave expansion is used, whereas inside the atomic sphere it is a combination of radial functions and spherical harmonics of the solution of the single electron Schrodinger equation. For exchange and correlation effects, the method of generalized gradient approximation (GGA) parameterized by Perdew, Burke, and Ernzerhohf (PBE96) [19] is used. Parameter RK_{max} of 7 is used in the simulation where R is the smallest atomic sphere radius in the unit cell and K_{max} is the magnitude of the largest K vector. RK_{max} will determine the matrix size used in self-consistency iterations. Lattice parameters for the $YTaO_4$ and $YNbO_4$ host lattices are taken from experimental data in Table 1. For integrals over the Brillouin zone, 18 k-points are used, as was implemented in [7].

The quantum effects contributed by strongly correlated d or f-electrons can be properly

treated using the GGA+U approach. There are two types of input parameters in the GGA+U calculation, namely U and J. U is the Hubbard energy or Coulomb parameter, while J refers to the exchange parameter. J is set to zero throughout the simulation. A different value of U will return a different output. The value of U is manually tuned until the resultant band gap from the GGA+U calculation agrees with that obtained by the experiments. The self-interaction corrected (SIC) variant of the GGA+U approach, which was introduced by Anisimov et al. [20], with an approximate correction for the self-interaction is used.

3. Results and discussion

3.1. Crystallographic data

Crystallographic structure of M′ $YTaO_4$ was first described by Wolten [21] with an "R" value of only 0.15. Later on Brixner and Chen [22] were able to reduce the "R" value to 0.034 and confirm the structure. It consists essentially of cube-like 8 coordinated Y polyhedra which can best be described as distorted square antiprisms. The average Y–O distance is 2.355 Å. The tantalum atoms are in a distorted octahedral coordination with four shorter Ta–O bonds at 1.86 and 1.95 Å, and two longer ones at 2.23 Å. The unit cell parameters are a = 5.30, b = 5.45, c = 5.11 Å and β = 96.5°.

The chemistry, as well as the structures of different tantalate's forms, are quite complex and for the purpose of the present article we shall restrict our discussion to the M′ form of $YTaO_4$, as it is the only structure exhibiting superior luminescent properties.

In the $YNbO_4$ host lattice, the niobium atom can be considered tetrahedrally coordinated to the oxygen atoms in a highly distorted site. In M-fergusonite, $YNbO_4$, this is no longer valid, since two of the four next-nearest oxygen ions are at shorter distance, whereas the other two are at longer distance than in the scheelite structure. We have to take into account the interaction between the Nb^{5+}- ion and six oxygen ions, i.e., to consider a Nb^{5+}- ion with a [4+2] coordination. From this point of view, the M-fergusonite structure is in between the scheelite structure with isolated tetrahedral groups and crystal structures of niobates with octahedral niobate groups [2–5, 22].

We took into account the atomic positions and lattice parameters in $YTaO_4$ and $YNbO_4$ mentioned in the cited above references, but the crystallographic data of investigated samples can vary a little from database results due to different sample synthesis and need to be carefully measured for particular samples when comparing crystallographic and luminescent properties. Therefore, we conducted XRD experiments for our samples independently. Our XRD measurements for prepared samples show the monoclinic phases of both phosphors (Fig. 1).

The detailed main peaks of synthesized tantalate phosphors in a range of 15°-50° are shown in Fig. 2b. From this figure it is evident that traditional XRD measurements with Cu-Kα radiation give wide peaks. To correctly determine the crystalline structures of the synthesized phosphors, we carried out XRD measurements on the basis of Synchrotron X-ray Diffraction patterns (Pohang Accelerator Laboratory, Korea). The result is shown in Fig. 2a. Similar results (not shown here) were also registered for niobate crystals.

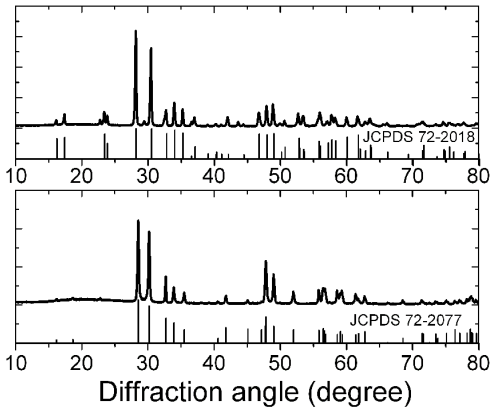

Fig. 1. XRD measurements (Cu-Kα radiation with λ = 1.54 Å source generated from a Rigaku rotating anode generator) of $YTaO_4$ phosphor (top) and $YNbO_4$ (bottom).

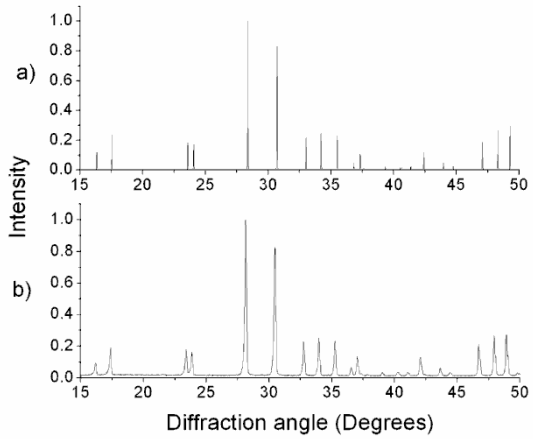

Fig. 2. A comparison of XRD measurements of $YTaO_4$ phosphor on the basis of synchrotron X-ray diffraction patterns (top) and Cu-Kα radiation (λ = 1.54 Å) source generated from a Rigaku rotating anode generator (bottom).

The Rietveld calculation provides the crystallographic information by comparing the model profile with X-ray or neutron curves using the least squares method. The lattice parameters and atomic positions from Rietveld analysis are presented in Table 1.

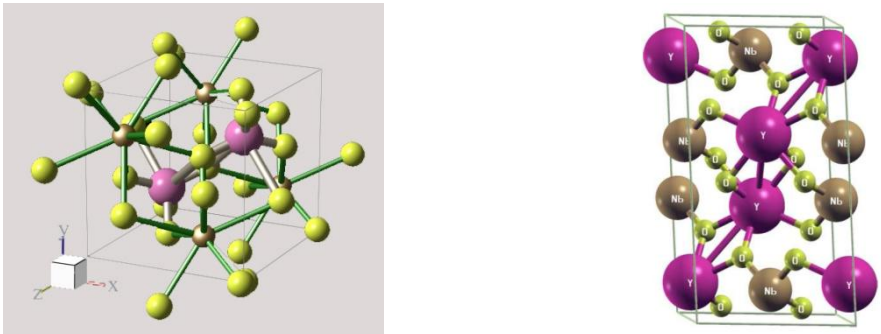

(a) (b)

Fig. 3. Crystal structure of M'- $YTaO_4$ (a) and $YNbO_4$ (b)

Table 1. Atomic positions and lattice parameters in $YTaO_4$ and $YNbO_4$

M'-$YTaO_4$	*Atom*	*x*	*y*	*z*	*F*
a=5.29568Å	Y	0.25	0.76523	0	1
b=5.445447Å	Ta	0.25	0.30632	0.5	1
c=5.10940Å	O(1)	0.49619	0.43402	0.27800	1
β=96.39119	O(2)	0.09912	0.09079	0.24181	1
M-$YNbO_4$	*Atom*	*x*	*y*	*z*	*F*
a=7.61851Å	Y	0	0.37891	0.25	1
b=10.94611Å	Nb	0	0.85620	0.25	1
c=5.29745Å	O(1)	0.20166	0.78039	0.20515	1
β=138.43617	O(2)	0.25050	0.96246	0.65526	1

These results are very close to those cited in Brixner and Chen [22]. One can see that the occupation factor $F = 1$, which means the site is fully occupied by an atom. The crystal structures of M'- $YTaO_4$ and $YNbO_4$ based on Table 1 are presented in Fig. 3.

3.2 Ab initio calculations, DOS and luminescence of $YTaO_4$

Figure 4 shows the DOS and band structure plots for $YTaO_4$ with and without considering *U*.

The coordinates of the special points used in plotting the $YTaO_4$ band structure are listed in Table 2.

Table 2. Coordinates of the special points used in plotting the band structure in Fig. 4

Label	Coordinates
GM	0,0,0
Z	0, 1/2, 0
Y	1/2, 0, 0
A	-1/2, 0, 1/2
B	0, 0, 1/2
D	0, 1/2, 1/2
E	-1/2, 1/2, 1/2

These coordinates can be obtained from standard sources, such as the Bilbao Crystallographic Server [23]. The band gap without Hubbard energy adjustment is 4.225 eV (Fig. 4a), while that with fine-tuned GGA+*U* is 5.15 eV (Fig. 4c). To obtain Fig. 4c and Fig. 4d, we vary the Hubbard energies *U* associated with the d-electrons of the Y and that of the Ta atom, respectively. We observe that when we "switch on" the Hubbard energy terms of either Y or Ta, or both, the band gap widens. While tuning for the best values of *U* for the Y and Ta atoms in a trial-and-error manner, we found that when *U* (Y atom)>*U* (Ta atom), the DOS of the Y atom will *overshadow* that of the Ta atom in the conduction region. Adding the exchange parameter *J* to the system will only make the band gap smaller but the overall DOS profile is almost unperturbed. Putting all these considerations together, the best values to match with the experimental findings are: *U* (Y atom) = 4.08 eV, *U* (Ta atom) = 11.56 eV, *J* (for both Ta and Y) = 0 eV. The band gap obtained with these *U* values is 5.15 eV. The Hubbard energy *U* provides a way to tune the output of the ab initio calculation to match the

energy gap as measured in the experiments. It is to be mentioned that the objective of tuning for the best values of *U* and *J* is not merely to match the band gap between experiment and ab initio calculation. Rather, the best values of *U* and *J* are used in the calculation of density of states (DOS) which are then compared with experiments.

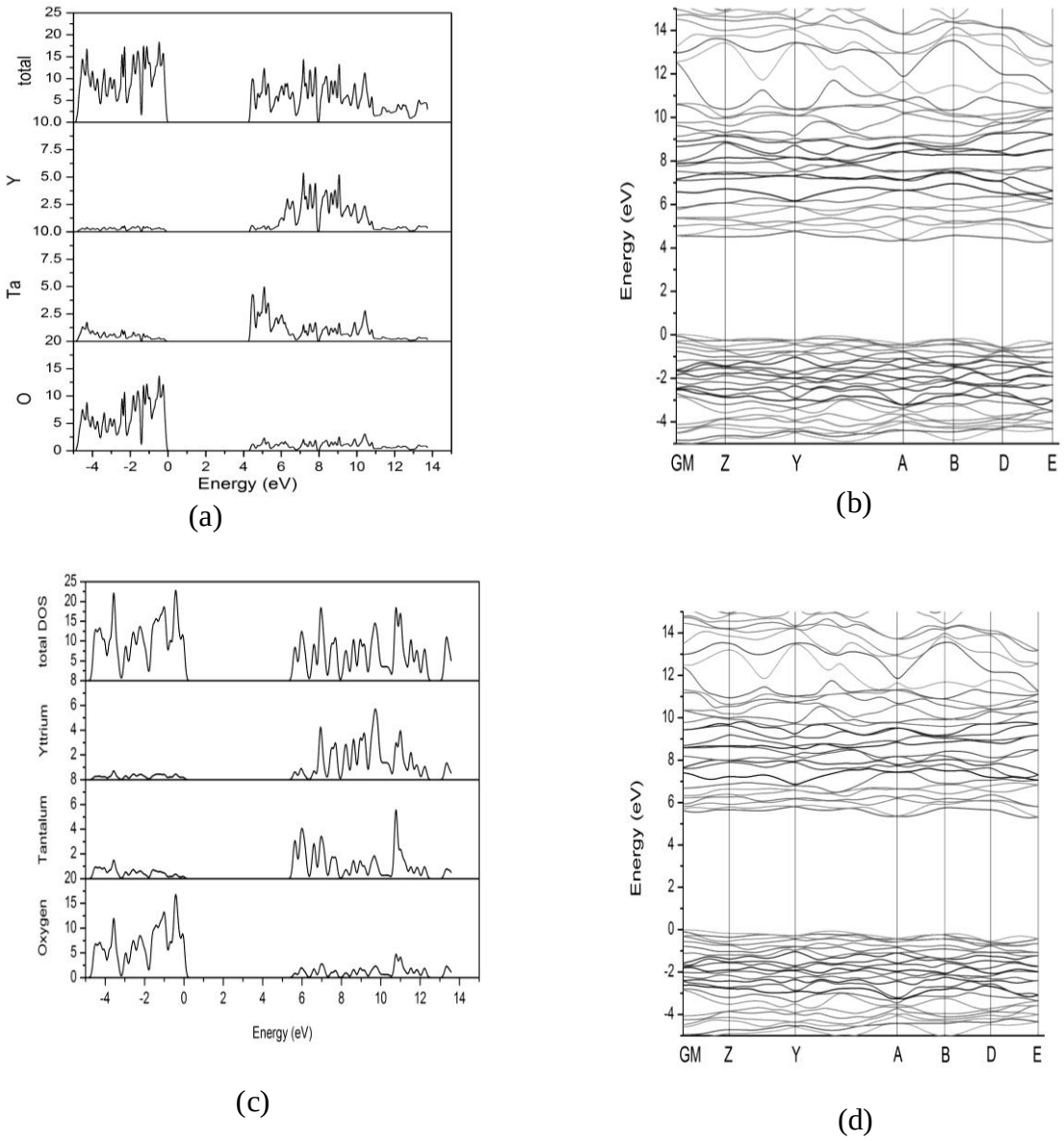

Fig. 4. (a) DOS and (b) band structure plot for $YTaO_4$ without considering Hubbard energy. (c) DOS and (d) band structure obtained with a fine-tuned Hubbard energy.

Although the values of the band gaps calculated by density functional theory are known to be underestimated [24], it is interesting to compare the gaps taken from the luminescence and absorbance experiments with calculated data. The results are compiled in Table 3. Band gap can be directly derived from absorbance spectra, such as that shown in Fig. 5, by determining the absorbance edge. The band gap value of 5.1 eV, as suggested from Fig. 5 (1) for $YTaO_4$, is in

good agreement with other experimental results listed in Table 3.

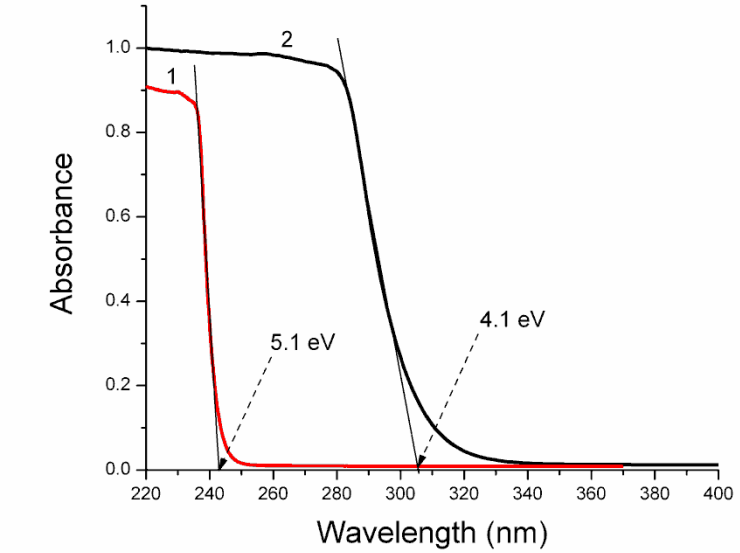

Fig. 5. Experimental absorbance spectra of $YTaO_4$ and $YNbO_4$ as measured in [25]. The band gaps deduced from this spectrum are 5.1 eV and 4.1, respectively.

Table 3. Reported band gap energies of $YTaO_4$

No.	E_{gap} (eV)	Method	Ref.
1	4.8	DFT (GGA method)	[10]
2	3.8	DFT (LDA method)	[7]
	5.0	Excitation spectrum	
3	5.2	DFT (GGA + scissor operator)	[25]
4	5.5	Abstracted from table 4.17 of Ref. [25]	[26]
5	3.8	Diffuse reflectance	[27]
6	5.0	Excitation spectrum	[28]
7	5.0	Excitation spectrum	[29]
8	5.1	Optical absorption spectrum	[30]
9	5.2	Optical absorption spectrum	[31]
10	5.4 5.0	Diffuse reflection spectrum Excitation spectrum	[32]
11	4.2	Calculated from DOS (GGA and LDA) using data from [30]	[33]
12	5.1	From absorption spectrum	This work
13	5.15	DFT (GGA+*U*)	This work

Figure 6 shows the PLE intensity measured experimentally and partial DOS of Y and Ta calculated from GGA+*U*.

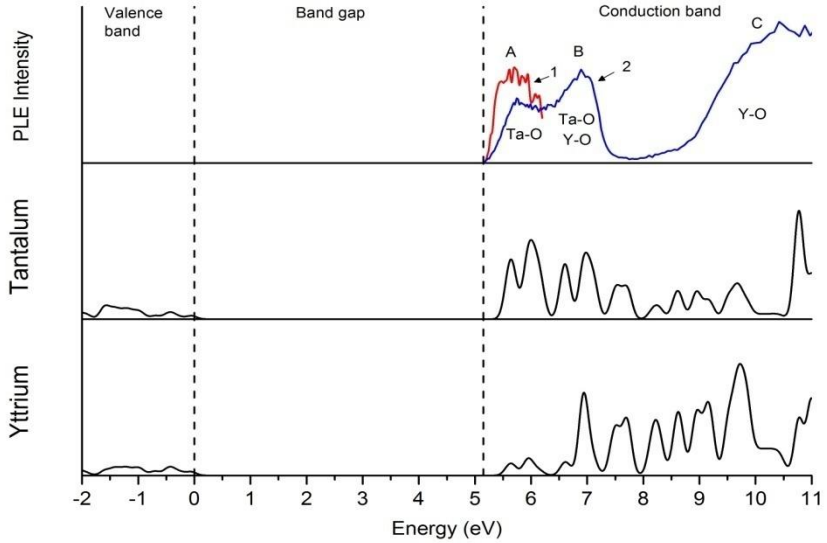

Fig. 6. UV (*1*) and VUV (*2*) excitation spectra of $YTaO_4$ with partial DOS of Y and Ta in the conduction band.

From the luminescence excitation spectra, the band gap in $YTaO_4$ corresponds to 5.15 eV and there are three bands A, B and C peaked around 6, 7, and 10 eV in the conduction band. The calculated partial DOS provides very insightful information to understand the characteristic features of these bands, such as identifying and explaining the nature of excitation bands and determining correctly the band gap in $YTaO_4$. In order to explain the nature of the A, B, and C bands in Fig. 6, we compare the PLE spectra against the calculated DOS. In Fig. 6, the position of the calculated conduction band on the energy scale was aligned with real spectra for the sake of easy comparison. As will be discussed below, the calculated DOS of the tantalum and yttrium provide a basis to understand the nature of bands A, B, and C in the excitation spectra.

Band A in the UV (*1*) and VUV (*2*) PLE around 6 eV in Fig. 6 can be associated with the absorption of the host lattices. The TaO_4^{3-} group can absorb excitation energy through $O^{2-} \rightarrow Ta^{5+}$ host charge transfer transition. This assumption is confirmed clearly by tantalum DOS distribution. The yttrium contribution in this area is negligible.

Band B in the VUV PLE spectra is also associated with the absorption of the host lattice, which involves mostly through $O^{2-} \rightarrow Ta^{5+}$ host charge transfer transition as well as the transitions between 4d-like states of Y and 2p-like states of O or Y^{3+}-O^{2-} (Fig. 6). Band B is a hybrid band, and it is composed from both [Y-O] and [Ta-O] charge transfer transitions.

Band C, peaked around 10 eV, is mostly related to the transitions between 4d-like states and 4s-like states of Y and 2p-like states of O. The Y-O bonds are excited and the energy is transferred to host lattice while the contribution of Ta-O is diminished.

If the high energies X-ray, electron beam, or VUV excitations were applied, it would be quite reasonable to assume that the excitation energy is absorbed first by the host lattice, which involves the transition between 4d-like states of Y and 2p-like states of O. The absorbed energy may then be transferred to TaO_4 groups and last transferred to the activator center, if any.

3.3 Ab initio calculations, DOS and luminescence of $YNbO_4$

As in previous paragraph, we use here the same DFT package WIEN2k to perform the GGA+U calculation for niobate system. Lattice parameters for the host lattice $YNbO_4$ are listed in Table 1. 18 k-points are used for integrals over the Brillouin zone. RK_{max} value is set to 7.

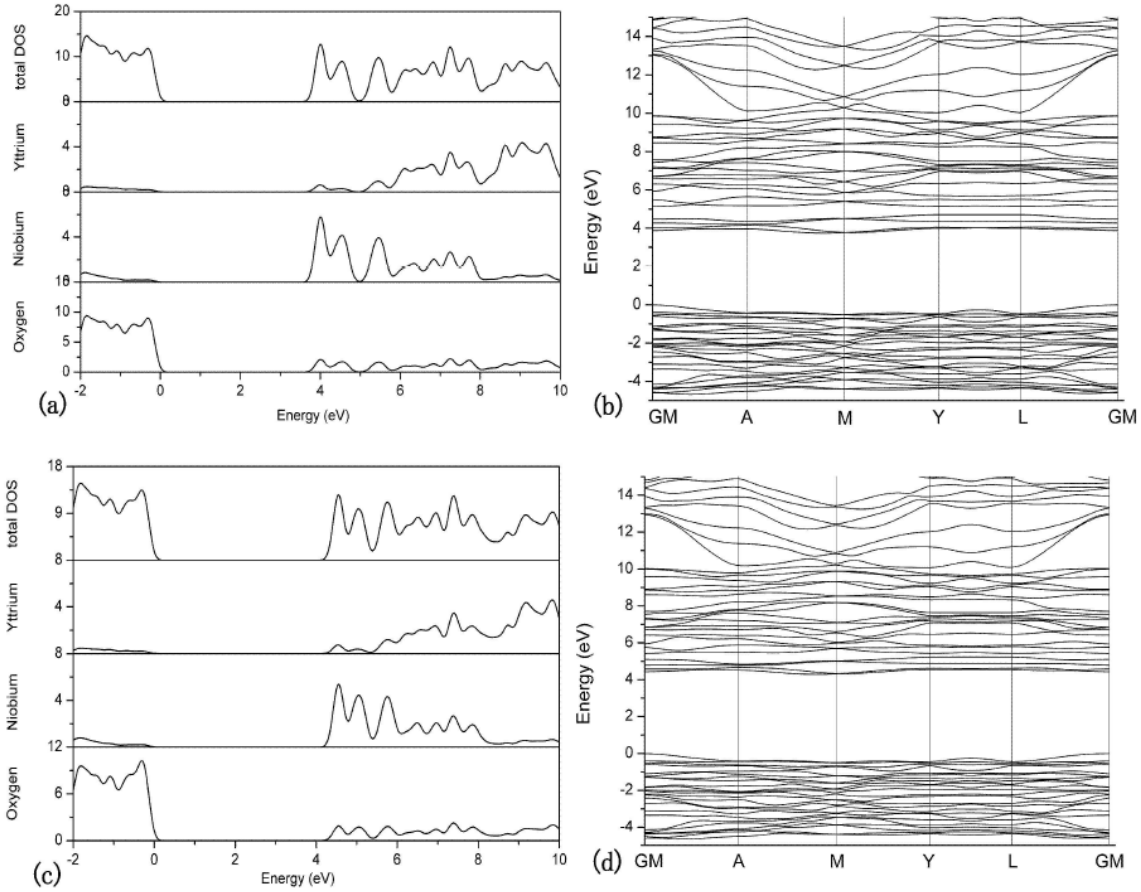

Fig. 7. (a) DOS and (b) band structure plot for $YNbO_4$ without considering Hubbard energy. (c) DOS and (d) band structure obtained with a fine-tuned Hubbard energy.

Figure 7 shows the DOS and band structure plot for $YNbO_4$ with and without considering Hubbard energy U. The band gap without Hubbard energy adjustment is 3.8 eV (Fig. 7a) while that with fine-tuned GGA+U is 4.28 eV (Fig. 7c). To obtain Fig. 7c and Fig. 7d, we vary the Hubbard energies U associated with the d-electrons of the Y and that of the Nb atom, respectively. Once the Hubbard energy U of the atom Y or Nb, or both, is switched on, the band gap widens. In the trial-and-error approach searching for the best values for U for the Y and Nb atoms, the DOS of the Y atom will overshadow that of the Nb atom in the conduction region unless U (Y atom) < U (Nb atom). Considering all the constraints, the best values to match with the experimental findings are: U (Y atom) = 0.68 eV, U (Nb atom) = 6.80 eV and the band gap obtained with these U values is 4.28 eV.

The DOS profile computed with fine-tuned Hubbard energy is almost identical with that computed without, except that the width of the band gap is varied with the strength of U. It thus can be concluded that the main effect of the Hubbard energy U on top of the GGA calculation on

this system is to widen the band gap, which in turn provides a way to tune the output of the ab initio calculations to match the energy gap as measured in the experiments. Band gap can be directly derived from absorbance spectra, such as that shown in Fig. 5, by determining the absorbance edge. The band gap value of 4.1 eV, as suggested from Fig. 5 (2) for $YNbO_4$, is in good agreement with other experimental results listed in the literature, which has a value lying between 4.1–4.4 eV [10, 25, 26, 34–40]. A similar result of ≈ 4.2 eV is estimated from excitation UV and VUV spectra as shown in Fig. 8.

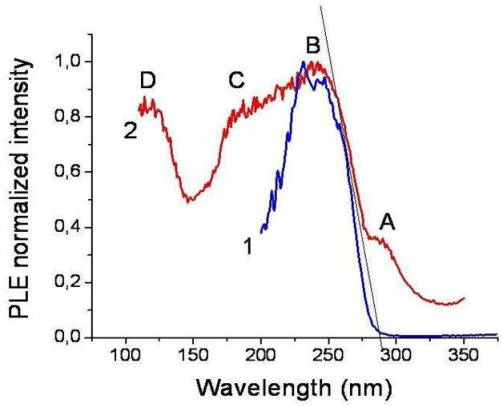

Fig. 8. PLE spectra for $YNbO_4$ under UV (*1*) and VUV (*2*) excitation.

To give a reliable interpretation to the overall feature of the luminescence and structural properties of niobate system, we investigate the excitation spectra of these materials and explain them from DOS theory. Four obvious large bands A, B, C, and D in the VUV PLE (Fig. 8) spectra are observed. We note that band A is only observed in the VUV but not in the UV data. We seek to clarify the nature of these bands with the aid from the DFT results. It is believed that bands B, C, and D in the VUV range in the niobate system are related to the following processes. Band B around 230 nm, which coincides well with the UV data, is associated with the absorption of the host lattices. The NbO_4^{3-} groups can absorb excitation energy through $O^{2-} \rightarrow Nb^{5+}$ host charge transfer transition. Bands C and D, peaking around 170 nm and 125 nm, are probably related to the host absorption. The Y-O bonds are excited and the energy is transferred to the host lattice.

The position of this band C for Y^{3+} ions can be calculated with the help of an empirical formula given by Jorgensen [41]

$$E_{CT} = [(X) - (M)] \times 30,000 \text{ cm}^{-1}.$$

Here, E_{CT} gives the position of the charge transfer band (CTB) in cm^{-1}, (X) the optical electronegativity of the anion, and (M) that of the central metal ion. Using the Pauling scale for electronegativity [42], namely (O)=3.44 and (Y)=1.22, the CTB of Y-O can be estimated near the 67.000 cm^{-1}, or around 150–160 nm.

To check this assumption and to explain the real nature of the bands, we compare the PLE spectra with the DOS calculated from first-principles (see Fig. 9).

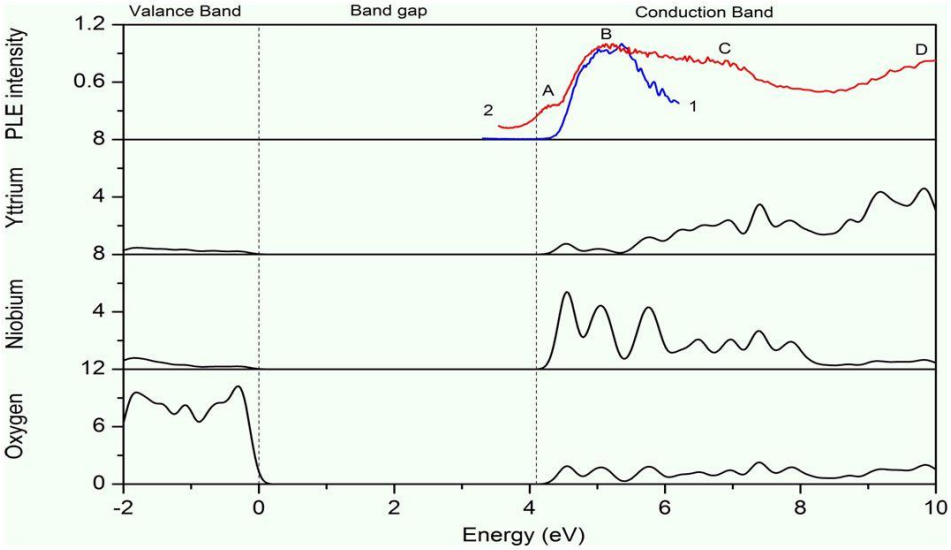

Fig. 9. UV (*1*) and VUV (*2*) excitation spectra of $YNbO_4$ with partial DOS of Y and Nb in the conduction band.

In the energy scale, the position of the calculated conduction band is aligned with real spectra. The contributions of Nb and Y are taken from partial DOS. The partial DOS of Niobium and Yttrium in Fig. 9 provides very insightful information to understand the characteristic features of these bands, such as identifying and explaining the nature of excitation bands and determining correctly the band gap in $YNbO_4$.

The nature of all the bands in excitation spectra can be explained by the Niobium and Yttrium partial DOS. Band A is partially located in the band gap. From DOS calculations for ideal structures, no contribution from Nb, Y, or O is observed in this area. Moreover, this band in UV spectrum for λ_{em} = 400 nm is not observed. It is thus supposed that band A is related to defects that can be excited by other wavelengths, because the excitation spectra in VUV were obtained by observing all emission light. The other possibility may be the calibration function in VUV measurements. The photoluminescence excitation spectra were measured in the VUV range of 100–350 nm using a sodium salicylate powder as a reference and calibrated by that of sodium salicylate, which has constant quantum efficiency in a range of 115–300 nm, and some artifacts can be seen in the ends of this area.

Band B in Fig. 9 is explained through the $O^{2-} \rightarrow Nb^{5+}$ host charge transfer transition. For the niobate system, the filled orbitals are concentrated on the oxygen ions and the empty ones on the niobium ions, so that the lowest optical transitions can be considered as 2p(O)→ 4d(Nb) charge transfer transitions. Thus, the excited state consists of an increased electron density in the vicinity of the metal ion along the tetrahedral bonds.

Band C is a hybrid band, and it is composed from both citation [Y-O] and [Nb-O] charge transfer transitions. Band D in the VUV PLE spectra is associated with the absorption of the host lattice, which involves mostly the transitions between 4d-like states of Y and 2p-like states of O or Y^{3+}- O^{2-} charge transfer transition.

If the high energies X-ray, electron beam or VUV excitations are applied, it would be quite reasonable to assume that the excitation energy is absorbed first by the host lattice, which involves the transition between 4d-like states of Y and 2p-like states of O. The absorbed energy

may then be transferred to NbO_4 groups and last transferred to the activator center, if any.

Using real UV excitation (Fig. 8, curve *1*) and emission spectra of $YNbO_4$ host lattice, as well as DOS interpretation (Fig. 9), the configurational coordinate diagram showing the energy transfer from excited to ground state is presented in Fig. 10.

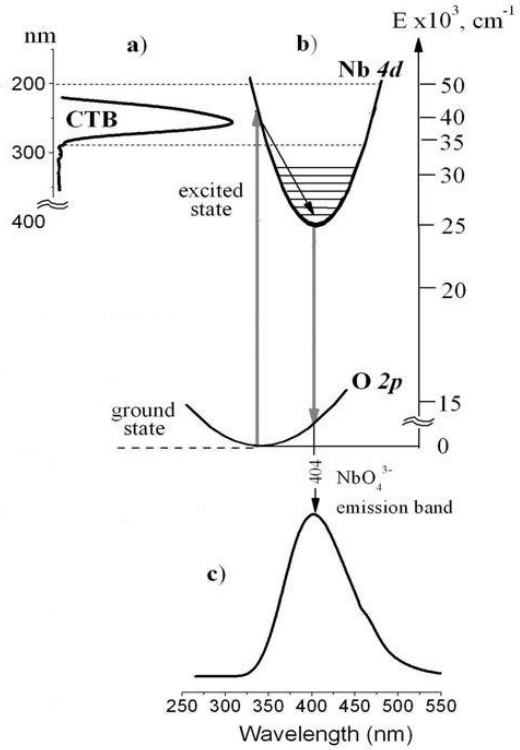

Fig. 10. Excitation (a) and emission (c) spectra of $YNbO_4$ host lattice and configurational coordinate diagram (b) corresponding to real data and showing the energy transfer from excited to ground state.

4. Conclusions

Through the GGA+U method as implemented in WIEN2k, we have addressed the band gap issue and the contribution of d-electrons from Y and Ta or Nb atoms in the conduction band. The band gap of the $YTaO_4$ host lattice is about 5.1 eV based on absorption and luminescence experiments, while the band gap of the $YNbO_4$ host lattice from DOS calculation is 4.28 eV and agrees well with 4.1 eV from absorption and luminescence experimental data. The band gap calculated using GGA+U is tuned to match the value from experiments by varying the Hubbard energies U associated with the Y and Ta or Nb atoms. The Hubbard energy U plays a major role in tuning the energy band gap to the right value. The J parameter, on the other hand, does not affect the calculation. Our GGA+U calculation shows that Ta atoms contribute to the total DOS in the 5–7 eV range for the tantalate system and Nb atoms in the 4–6 eV range for the niobate system, while Y atom dominates from 7eV onwards in the conduction band for both. These results are in good agreement with the luminescence experiment and explain well the three bands as measured in the UV and VUV excitation spectra.

References

[1] R. B. Ferguson, Can. Mineral 6, 72 (1957).
[2] J. M. Jehng and I. E. Wachs, Chem. Mater. 3, 100 (1991).
[3] A. H. Buth and G. Blasse, Phys. Stat. Sol. (a) 64, 669 (1981).
[4] M. J. J. Lammers and G. Blasse, Mater. Res. Bull. 19, 759 (1984).
[5] V. S. Stubican, J. Am. Ceram. Soc. 47, 55 (1964).
[6] M. Nazarov, D. Y. Noh, A. Zhbanov, and Y.-G. Lee, J. Ceram. Process Res. 12, s183 (2011).
[7] D. Xiang, B. Liu, M. Gu, X. Liu, S. Huang, and C. Ni, Acta Optica Sinica. 29, 448 (2009).
[8] I. D. Arellano, M. Nazarov, and D. Y. Noh, Rev. Colomb. Fisica. 41, 123 (2009).
[9] I. Arellano, M. Nazarov, C. C. Byeon, E.-J. Popovici, H. Kim, H. Y. Kang, and D. Y. Noh, Mater. Chem. and Phys. 119, 48 (2010).
[10] M. Nazarov and A. Zhbanov, Mold. J. Phys. Sci. 10, 52 (2011).
[11] K. Terakura, T. Oguchi, A. R. Williams, and J. Kubler, Phys. Rev. B, 30, 4734 (1984).
[12] V. I. Anisimov, J. Zaanen, and O. K. Andersen, Phys. Rev. B, 44, 943 (1991).
[13] V. I. Anisimov, F. Aryasetiawan, and A. I. Lichtenstein, J. Phys: Condens. Matter. 9, 767 (1997).
[14] A. I. Lichtenstein, J. Zaanen, and V. I. Anisimov, Phys. Rev. B, 52, R5467 (1995).
[15] P. Blaha, K. Schwarz, G. Madsen, D. Kvasnika, and K. Luitz, Wien2k, Technical Universitat Wien, Austria, 2001. ISBN 3-9501031-1-2.
[16] D. J. Singh, Plane Waves, Pseudopotential and the LAPW Method, Kluwer-Academic, Boston, 1994.
[17] E. Wimmer, H. Krakauer, M. Weinert, and A. J. Freeman, Phys. Rev. B, 24, 864 (1984).
[18] M. Weinert, E. Wimmer, and A. J. Freeman, Phys. Rev. B, 26, 4571 (1982).
[19] J. P. Perdew, K. Burke, and M. Ernzerhof, Phys. Rev. Lett. 77, 3865 (1996).
[20] V. Anisimov, I. Solovyev, M. Korotin, M. Czyzyk, and G. Sawatzky, Phys. Rev. B, 48, 16929 (1993).
[21] G. M. Wolten, Acta Crystallogr. 23, 939 (1967).
[22] L. H. Brixner and H. Y. Chen, J. Electrochem. Soc. 130, 2435 (1983).
[23] Bilbao crystallographic server, http://www.cryst.ehu.es/cgi-bin/cryst/programs/
[24] M. S. Hybertsen and S. G. Louie, Phys. Rev. B, 34, 5390 (1986).
[25] M. Nazarov and D. Y. Noh, New Generation of Europium and Terbium activated Phosphors, Pan Standford Publishing, 2011.
[26] A. H. Krumpel, P. Boutinaud, E. van der Kolk, and P. Dorenbos, J. Lumin. 130, 1357 (2010).
[27] M. Liu, W. You, Z. Lei, G. Zhou, J. Yang, G. Wu, G. Ma, G. Luan, T. Takata, M. Hara, K. Domen, and C. Li, Chem. Commun. 2192 (2004).
[28] Li Bo, G. Zhen-nan, D. Yi, L. Jian-hua, and S. Mian-zeng, Chem. Res. Chin. Univers. 15, 226 (1999).
[29] Hubin, H. Huangyan, G. Shucai, and Kongli, Chin. J. Lumin. 30, 601 (2009). (in Chinese).
[30] L. Kazakova, A. Dubovsky, G. Semenkovich, and O. Ivanova, Radiat. Meas. 24, 359 (1995).
[31] L. Kazakova, I. Bykov, and A. Dubovsky, J. Lumin. 72–74, 211 (1997).
[32] G. Blasse, A. Bril, J. Lumin. 3, 109 (1970).
[33] H. Hori, T. Kobayashi, R. Miyawaki, S. Matsubara, K. Yokoyama, and M. Shimizu, J. Mineral. Petrolog. Sci. 101, 170 (2006).

[34] G. Blasse and A. Bril, J. Chem. Phys. 48(1), 217 (1968).
[35] S. K. Lee, H. Chang, C. H. Han, H. J. Kim, H. G. Jang, and H. D. Park, J. Solid State Chem. 156(2), 267 (2001).
[36] X. Xiao and B. Yan, J. Alloys and Compd. 421, 252257 (2006).
[37] C. Han, H. Kim, H. Chang, S. K. Lee, and H. D. Park, J. Electrochem. Soc. 147(7), 2800 (2000).
[38] S. H. Shin, D. Y. Jeon, and K. S. Suh, J. Appl. Phys. 90(12), 5986 (2001).
[39] A. Massabni, G. Montandon, and M. C. D. Santos, Mater. Res. 1, 01 (1998).
[40] Y. Zhou, Q. Ma, M. Lu, Z. Qiu, and A. Zhang, J. Phys. Chem. C 112(50), 19901 (2008).
[41] C. K. Jorgensen, Prog. Inorg. Chem. 12, 101 (1970).
[42] L. Pauling, Nature of the Chemical Bond, 3rd ed. (Cornell University Press, 1960).